RESEARCH ARTICLE

Treatment of simulated electroplating wastewater containing Ni(II)-EDTA by Fenton oxidation combined with recycled ferrite process under ambient temperature

Lei Wang[1,2] · Zhijun Luo[1] · Jing Wei[1] · Xiangtong Zhou[1] · Xiaoying Zhang[1] · Huicheng Ni[1] · Jing Wang[1] · Youye Song[1] · Zhiren Wu[1]

Abstract

Developing low cost and efficient method for the treatment of electroplating wastewater containing heavy metals complexed with chelating agent has attracted increasing attention in industrial wastewater treatment. This study involved a system combining Fenton oxidation (FO) and recycled ferrite (RF) process for treating synthetic solution containing Ni(II)-EDTA at ambient temperature. In this system, the FO reaction can produce hydroxyl radicals with high redox potential to decomplex the metal-organic complexes and degrade the organics, thereby enhancing the removal efficiency of heavy metals. The RF process is to incorporate the non-iron metal into the spinel ferrites at room temperature, and stabilize the sludge. As a result, the toxicity characteristic leaching procedure can fulfill the relevant standards. Furthermore, the ferrous ions in Fenton reaction could be used as the source of irons in RF process. After treatment by the combined process, the effluent water fulfills the relevant standard in China. In comparison with conventional alkaline precipitation, the sludge sedimentation velocity of FO-RF is 2.16 times faster than that of conventional alkaline precipitation and the volume of sludge is reduced by half, which strongly demonstrated the advantages of the presented FO-RF system and indicated the huge potential for the treatment of EDTA-chelated nickel.

Keywords Fenton oxidation · Ferrite · Ni(II)-EDTA · Sludge performance

Introduction

Electroplating wastewater contains different kinds of heavy metals, chelating agents (e.g., ethylenediaminetetraacetic acid, EDTA), spent acids, and other inorganic as well as organic species. It is harmful to the environment and human health and the
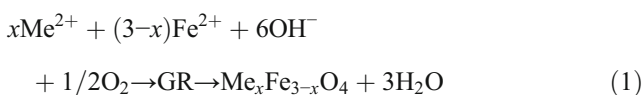
✉ Zhijun Luo
lzj@ujs.edu.cn

✉ Zhiren Wu
wuzhiren@ujs.edu.cn

[1] School of the Environment and Safety Engineering, Jiangsu University, 301 Xuefu Road, Zhenjiang 212013, China

[2] School of Environmental Resources, AnQing Normal University, No.1318 Jixian North Road, Anqing 246133, China

increasing discharge of this heavy metal sewage has drawn increasing attention because of its non-biodegradability and high toxicity. Moreover, as a strong complexing agent, EDTA can not only enhance the mobility of heavy metals but can also make them refractory to the traditional methods. Nowadays, in order to mitigate heavy metal pollution, more and more stringent standards have been introduced to control discharge of electroplating wastewater. Therefore, it is urgent to establish effective technologies to solve this problem (Cunha Gda et al. 2015; Han et al. 2016; Wu et al. 2013; Yi et al. 2018, 2019a, b).

Traditional technologies including ion exchange (Kim et al. 2002; ShinJuang and ChunLin 2001), coagulation (Rincon and La Motta 2014), membrane adsorption separation (ShinJuang et al. 1999), and alkaline precipitation (Fu et al. 2012; Ju and Hu 2011; Lan et al. 2012; Xu et al. 2015) have been applied to treat wastewater containing heavy metals. Among them, alkaline precipitation method has been preferentially chosen due to its low-cost and simple operation, but it is also restricted by some disadvantages such as high sludge volume ratio and water content, loose structure of the resulting

precipitate, and slow separation. Moreover, the alkaline precipitation will unhinderedly redissolve under acidic conditions, and the result of sludge toxicity characteristic leaching procedure (TCLP) test cannot fulfill the demands. Therefore, stabilization/solidification process will be required before discharge. Several methods to stabilize the precipitate have been reported, including cement solidification (Koo et al. 2017) and chemically bonded phosphate ceramic (CBPC) technology (Kim and Lee 2017). But these methods may cause secondary pollution, and additional treatments will increase the costs.

The ferrite process (FP) is an established method for treating heavy metal wastewater by incorporating heavy metals into stable spinel-type structure (Erdem and Tumen 2004; Klas et al. 2011; Morgan et al. 2004). It has more merits than alkaline precipitation method such as efficient removal of metal ions, easy solid–liquid separation, and low cost. In addition, the performance of FP sludge was superior to that of traditional alkaline precipitation. It presented a lower water content, faster sedimentation velocity, appropriate chemical stability for solids disposal, soft magnetism, and dense structure. Additionally, the FP sludge could be recycled as magnetic material (Guivar et al. 2015; Hasanzadeh et al. 2015), energy storage (Chandra et al. 2015), and microwave device (Dar et al. 2016), as well as catalyst for steam reforming of methanol (Huang et al. 2015) and synthetic natural gas (Chen et al. 2017a). The removal mechanism of heavy metals in solution by FP is presented in Eq. (1). Non-iron metals (Me) and ferrous ions form an intermediate complex of colloidal structure called green rust (GR) after co-precipitating in alkaline condition. And dehydration processes convert the GR into a stable spinel ferrite. However, dehydration is the rate-limiting step in the process of ferrite formation which need a long aging time. Elevating temperatures (higher than 70 °C) can shorten the time of dehydration and promoted metal-bearing spinels stable structure generation (Lou and Huang 2009; Lou et al. 2009). However, the operating costs will also increase.

$$x\mathrm{Me}^{2+} + (3-x)\mathrm{Fe}^{2+} + 6\mathrm{OH}^-$$
$$+ 1/2\mathrm{O}_2 \rightarrow \mathrm{GR} \rightarrow \mathrm{Me}_x\mathrm{Fe}_{3-x}\mathrm{O}_4 + 3\mathrm{H}_2\mathrm{O} \quad (1)$$

In recent years, advanced oxidation processes (AOPs) including Fenton (Fu et al. 2009; Fu et al. 2012), UV/H$_2$O$_2$ (Xu et al. 2017), or photoelectrocatalytic oxidation (Chen et al. 2017b) have been widely reported for treatment of huge discharge of industrial wastewater containing organic metal complexes. Among them, Fenton oxidation (FO) is an effective technology for decomplexation owing to the strong oxidizing property (E^0 = 2.4–3.0 V) (Fu et al. 2009). It has been extensively employed to degrade metal-EDTA complexes accompanying the release of free metallic ions. The oxidized products such as O$_2$, OH$^-$, and H$_2$O are eco-friendly, and the process is easily operated and maintained. Therefore, the FO

method is an attractive and effective technology for the degradation of pollutants in industrial wastewaters. Besides, iron compound materials, including magnetite (Fe$_3$O$_4$) (Qiu et al. 2016) and spinel ferrites (Jiang et al. 2015; Qu et al. 2019), can be used as heterogeneous Fenton catalysts to decompose the organic compounds in industrial wastewater. It showed a good catalytic performance under neutral conditions.

In general, metal ions in electroplating wastewater usually exist in the form of chelated heavy metal, and this stable chelating structure seriously constrains the removal efficiency of metal ions. It is hard to treat this kind of industrial wastewater by single method. Furthermore, most of the electroplating wastewaters are highly acidic which provide the suitable environment for the Fenton reaction. Therefore, we proposed a new method combining FO with recycled ferrite (RF) process for the treatment of electroplating wastewater contained Ni(II)-EDTA at ambient temperature. Some advantages in solving abovementioned problems are as follows. First of all, the FO reaction could be used for decomplexing of metal-organic complexes. Second, in the degradation mechanism of pollutants, Fe(II) serving as catalysts indirectly participates in oxidizing target compounds (Fu et al. 2009). The ferrous ions in the effluent water after FO process could be used as the source of iron ions in the RF process. Moreover, there is no need to raise the temperature by advanced seeded ferrite method (RF). The resulting sludge is easily to be separated and stabilized without more additional stabilization treatments. At last, the magnetic ferrites in RF process can be used as catalysts to produce hydroxyl radical. As a result, the decomplexation of chelated metal was enhanced. Therefore, the objectives of this paper were to (i) investigate the initial parameters, including the dosages of Fe(II) and H$_2$O$_2$ and their effect on the removal of Ni(II)-EDTA by Fenton method, (ii) discuss the pH value, Ni/T-Fe, and returning slurry ratio which influence the proposed RF process, (iii) gain the number of iron ions (including ferrous and ferric iron) which entered the ferrite process after Fenton reaction, and (iv) evaluate the settleability and stability of the resulting sludge.

Materials and methods

Materials and reagents

Deionized water was used for the preparation and dilution of all solutions. All of the reagents were purchased from Sinopharm Chemical Reagent Co., Ltd. (Shanghai, China), except that (NH$_4$)$_3$PO$_4$·3H$_2$O were purchased from Zhiyuan Chemical Reagent Co., Ltd. (Tianjin, China). Ni(II)-EDTA solution was prepared by mixing NiCl$_2$·6H$_2$O and Na$_2$-EDTA·2H$_2$O with an equal molar ratio. pH of the solution was adjusted by 0.1 M HCl and 0.1 M NaOH prior to the

reaction. All reagents were of analytic grade and used without further purification.

Analytical methods

All water samples were withdrawn for analysis after filtration using a 0.22-μm mixed cellulose membrane. The total organic carbon (TOC) concentration was measured with a TOC-L (CPH/CPN, Japan) analyzer (Xu et al. 2017). The removal efficiency of TOC can be described as the Eq. 2. C_o (mg/L) and C_t (mg/L) represent the initial and residual TOC concentration at time t (min), respectively. The concentration of ferrous ions was monitored by the o-phenanthroline method (HJ/T 345-2007, China) at $\lambda = 510$ nm using DR3900 (HACH, America) (Lan et al. 2012). The amount of nickel was measured by inductively coupled plasma atomic emission spectrometry (ICP-AES, Japan). Ni(II)-EDTA was analyzed using a high-performance liquid chromatography (HPLC) system. C18 column (4.6 mm × 150, 5 μL) was used for the Ni(II)-EDTA separation. The mobile phase in HPLC consisted of a mixture of acetonitrile:phosphate buffer salt (ammonium phosphate, 20 mM) = 25:75 (v:v), and the pH of buffer salt solution was adjusted to 2.5 using phosphoric acid. Flow rate of 1.0 mL/min, column temperature of 25 °C, and the optimal detection wavelength of 210 nm were applied (Li et al. 2017).

$$R_{\text{TOC}} = \frac{C_0 - C_t}{C_0} \tag{2}$$

In order to prove the superiority of FO-RF method, ferrite sludge was compared with traditional alkaline precipitated sludge. Sludge performance evaluation including stable sludge volume ratio (R, %), compressed solid concentration (ρ, g/L), and water content (W_c, %) was evaluated using the following equations:

$$R = \frac{V_T}{V_S} \tag{3}$$

where V_S (L) and V_T (L) represent the concentrated sludge volume after 24 h and total volume, respectively.

$$\rho = \frac{M_S}{V_O} \tag{4}$$

where M_S (g) and V_o (L) represent the total concentrated sludge quality and the concentrated sludge volume after 24 h, respectively.

$$W_C = \frac{M_S - M_d}{M_S} \tag{5}$$

where M_d (g) represents the concentrated sludge quality after drying at 105 °C.

Stability of the resulting sludge was evaluated by TCLP with a standard method, as published in China (HJ/T 300-2007). In brief, the extraction agent containing 64.3 mL 1 M NaOH and 5.7 mL glacial acetic acid was mixed together in a 1-L volumetric flask. Then 1 g of resulting dry sludge is added into a 50-mL centrifuge tube, and 20 mL of extraction agent was added. The centrifuge tube was rotated for 18 ± 2 h in a shaking mixer. Each sample was centrifuged and filtered before measurement.

To further evaluate the performance of sludge, X-ray diffraction (XRD) (ADVANCE D8) analyses were measured to characterize the crystallization. A field emission scanning electron microscope (SEM) (FESEM S-4800 II) was used to observe the surface of resulting sludge. Energy dispersive spectrometer (EDS) was used to determine the sludge alloy composition. Transmission electron microscope (TEM) (Tecnai 12) was also used to observe the particle size of resulting sludge.

FO process for removing Ni(II)-EDTA

The Fenton oxidation process was carried out in 500-mL beakers with an agitator and pH meter. First, the beakers were filled with 200 mL Ni(II)-EDTA solution containing nickel concentration of 200.0 mg/L at ambient temperature. Then, H_2O_2 and Fe(II) were added into the Ni(II)-EDTA solution and mixed for 60 min. The initial pH was set at 2.5 in this study.

RF process for removing Ni(II)

In this study, the wastewater containing nickel was prepared using $NiCl_2 \cdot 6H_2O$, and continuously pumped into the RF reactor at a flow rate of 96 L/d. The solution in RF reactor was 4 L and reached a pH of 10. The speed of stirrer was maintained at around 100 rpm. Fe(II) ($FeSO_4 \cdot 7H_2O$, pH = 4) was directly added to the RF reactor by a peristaltic pump and the slurry was pumped into the RF reactor after pH adjustment in alkaline conditioning tank using 2 M NaOH solution. The initial seed was prepared by the ambient temperature procedure.

FO-RF process

The FO-RF process is operated continuously and the course of the wastewater treatment is depicted as follows. First, wastewater was prepared by mixing $NiCl_2 \cdot 6H_2O$ and Na_2-EDTA·$2H_2O$ with an equal molar ratio in the tank, which contained 3.4 mM Ni(II)-EDTA (pH = 2.5). $FeSO_4$ and H_2O_2 reagent batch-type entered into the FO reactor by peristaltic pump for Fenton reaction. Then, the effluent water of the FO was pumped into the RF reactor. Second, $FeSO_4$ solution (73 mM, pH = 4) and returning slurry from the alkaline conditioning tank were serially fed to the RF reactor by peristaltic pump. The oxidation reduction potential (ORP) and pH value in this

process were monitored. Finally, after separation in thickener, the effluent water and resulting sludge were collected for concentration analysis and sludge characteristics experiment, respectively. Overall, the removal efficiency of nickel and Ni(II)-EDTA by the FO-RF process was investigated (Fig. 1). TCLP, water content, compressed solid concentration, and settleability of the resulting sludge were determined and evaluated.

Results and discussion

FO process on removal of Ni(II)-EDTA

Effect of Fe(II) dosage

Fe(II) ion as catalyst plays a significant role in Fenton reaction. The effect of Fe(II) concentration on the removal efficiency of Ni(II)-EDTA by FO process was investigated with different dosage of Fe(II) ions in 1800 mg/L H_2O_2 solutions.

As shown in Fig. 2a, without the existence of Fe(II) ions, the efficiency of decomplexation by H_2O_2 was 21.5% after 60 min. With Fe(II) dosage of 300 mg/L, $R_{Ni(II)\text{-}EDTA}$ by FO was remarkably increased to 87.6%. The results indicated that the removal efficiency increased with higher Fe(II) concentration, due to generation of ·OH (Eq.(6)) (Zhou et al. 2016). It should be noted that further increasing Fe(II) dosage above 450 mg/L had slight influence on the efficiency, probably due to the self-scavenging of ·OH (Eq.(7)). Additionally, the total organic carbon (TOC) concentration was also analyzed, and Fig. S1a. illustrates that TOC concentration rapidly decreased with Fe(II) dosage enhanced from 150 to 300 mg/L at the beginning. As further increasing Fe(II) concentration to 450 mg/L, 72.2% TOC removal efficiency could be achieved. A comparison of the results of the two experiments (TOC and HPLC analysis) shows a very similar trend. Therefore, the concentration of 450 mg/L was chosen as the optimal dosage for the following experiments.
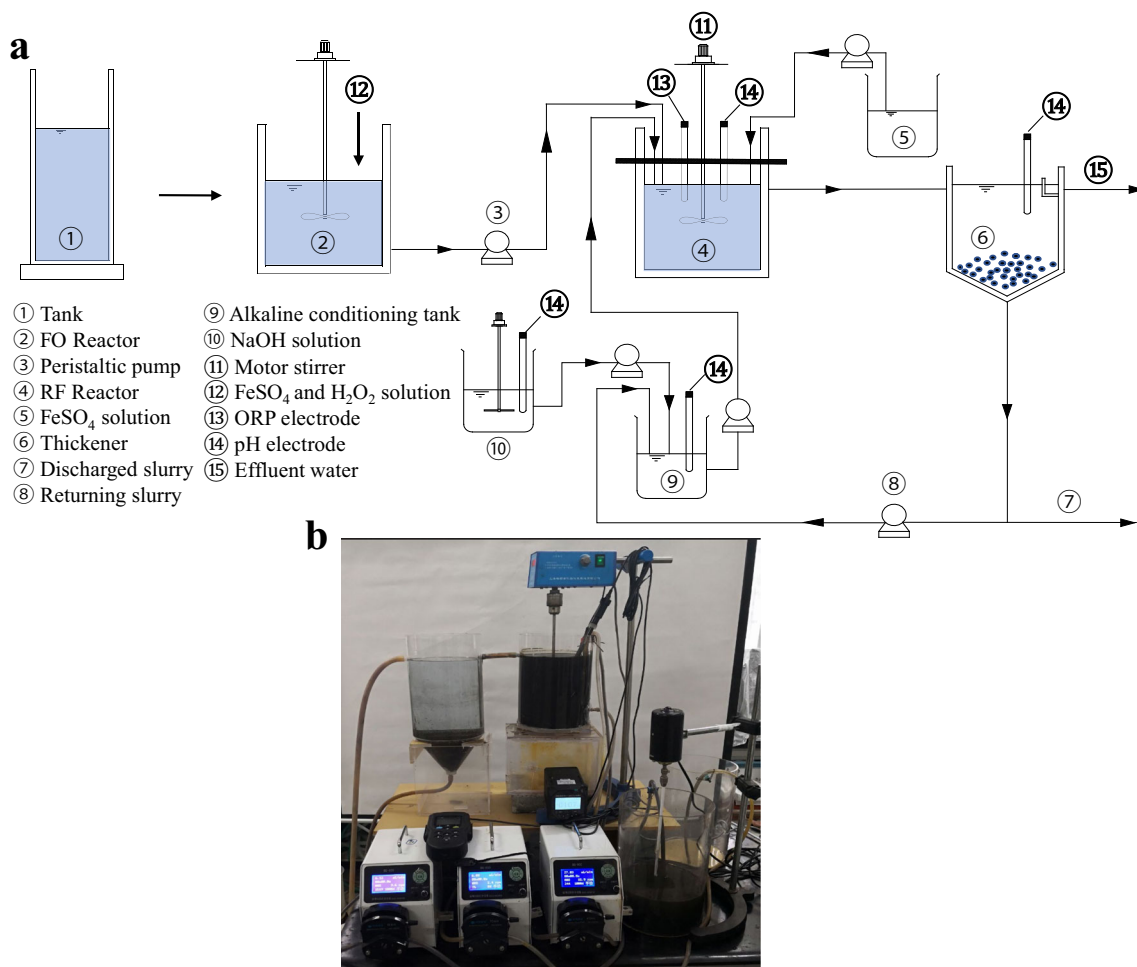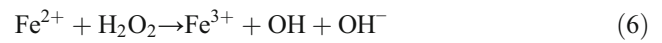
$$Fe^{2+} + H_2O_2 \rightarrow Fe^{3+} + OH + OH^- \tag{6}$$

① Tank
② FO Reactor
③ Peristaltic pump
④ RF Reactor
⑤ FeSO₄ solution
⑥ Thickener
⑦ Discharged slurry
⑧ Returning slurry
⑨ Alkaline conditioning tank
⑩ NaOH solution
⑪ Motor stirrer
⑫ FeSO₄ and H₂O₂ solution
⑬ ORP electrode
⑭ pH electrode
⑮ Effluent water

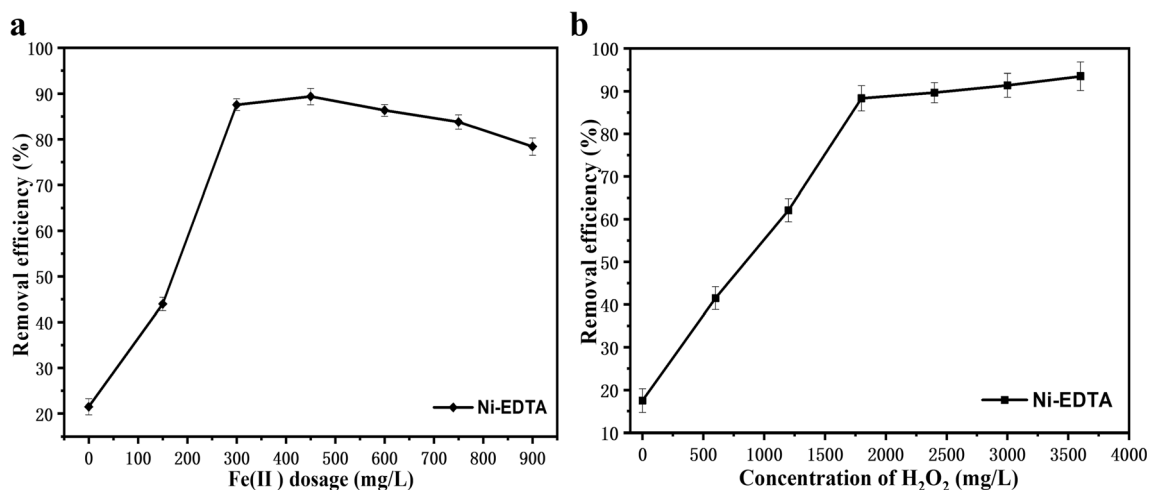**Fig. 1** **a** Schematic diagram of the FO-RF system and **b** picture of real products

Fig. 2 Effect of initial Fe(II) (**a**) and H_2O_2 (**b**) concentrations on removal efficiency of Ni(II)-EDTA by FO (pH$_0$ = 2.5, [Ni(II)-EDTA]$_0$ = 3.40 mM, and reaction time, 1 h)

$$Fe^{2+} + HO \cdot \rightarrow Fe^{3+} + OH^- \tag{7}$$

Effect of H_2O_2 concentration

Besides Fe(II), H_2O_2 is known to be another important component for ·OH generation. From the Fig. S1b., it can be concluded that TOC residual concentration reduced with the increase of the hydrogen peroxide. The degradation rate was fast with the H_2O_2 concentration from 600 to 1800 mg/L at the beginning. After that, it slowly increased once the dosage of H_2O_2 exceeds more than 1800 mg/L. The effect of H_2O_2 dosage on degradation of Ni(II)-EDTA was also investigated by HPLC, and the results are displayed in Fig. 2b. In the absence of H_2O_2 (the concentration of Fe(II) is 450 mg/L), the degradation efficiency of Ni(II)-EDTA is only 17.5%, which implies that the decomplexation of Ni(II)-EDTA mainly depends on H_2O_2 and its product (·OH). Without H_2O_2, the removal efficiency of Ni(II)-EDTA was attributed to the cooperation of the Fe(III) replacement as well as adsorption, while replacement was the main process (Ju and Hu 2011; Liu et al. 2017). In this research, Fe(II) ions may be partially oxidized to Fe(III) ions by oxygen (Eq.(8)), with Ni(II)-EDTA complexes converted into Fe(III)-EDTA (Eq.(9)). It is also observed that the removal efficiency of Ni(II)-EDTA increases from 17.5 to 88.3% with H_2O_2 concentration of 1800 mg/L; however, there was no significant improvement by further increasing the H_2O_2 concentration to 3600 mg/L. Thus, taking into account the operation and maintenance cost, the optimal concentration of H_2O_2 was set at 1800 mg/L.

$$4Fe^{2+} + O_2 + 2H_2O \rightarrow 4Fe^{3+} + 4OH^- \tag{8}$$

$$Fe^{3+} + Ni(II)-EDTA \rightarrow Fe(III)-EDTA + Ni^{2+} \tag{9}$$
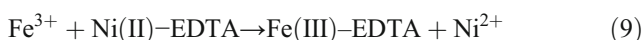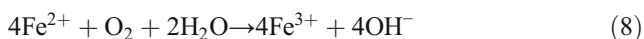
In previous work, Lan et al. have reported that the optimal [Fe(II)]/[H_2O_2] concentration ratio was 0.3 (Lan et al. 2012), which is similar with our experimental results of 0.25. The concentration of Fe(II) in FO effluent water was only 3.6–7.0 mg/L in the best condition, with an initial Fe(II) concentration of 450 mg/L. Most of Fe(II) had been oxidized to Fe(III) in FO process. The FO effluent water was then discharged into the RF reactor as the source of iron ions for ferrite process.

Results of recycled ferrite

pH value

Since pH is one of the most important influencing factors in RF process, the effect of pH on the treatment of containing nickel wastewater was investigated. The pH was controlled by pumping NaOH solution into the alkaline conditioning tank. When the pH of alkaline conditioning tank was adjusted, accordingly, the pH values of these two containers would also changed. The relevance of pH values in three containers is shown in Table 1. To figure out the effect of pH on the RF system, the concentration of nickel in effluent water from thickener supernatant and the TCLP test of the bottom sludge in thickener were measured (Fig. 3a). The phase of the sludge was also explored by XRD as shown in Fig. 3b.

As shown in Fig. 3a, the nickel concentrations in effluent water and TCLP test both decrease firstly and increase later with the increase of pH value. The minimum concentration of nickel both in effluent water and TCLP test is achieved at pH = 10.0. When the pH value increases from 7.4 to 10.0 in RF reactor, the concentration of nickel in effluent water reduces from 0.67 to 0.32 mg/L. At the same time, TCLP result of the resulting sludge decreases from 10.37 to 3.87 mg/L. Lower concentration of nickel in TCLP test can be achieved

Table 1 The pH value in different containers (mg/L)

Serial number	1	2	3	4	5	6
Alkaline conditioning tank	8.5	9.2	10.4	11.8	12.7	13.6
RF reactor	7.4	8.1	9.2	10.0	11.2	12.3
Thickener	5.8	6.7	7.6	8.5	10.1	11.2

at a higher pH value, probably owing to the incorporation of heavy metals into magnetite by forming ferrite in alkaline solution, which is also confirmed by XRD patterns in Fig. 3b. With the pH value increasing to 10, XRD patterns of the sludge shows a sharper ferrite peaks leading to a better crystallinity, which is also consistent with the result of TCLP test.

As the pH further increasing from 10.0 to 12.3, the concentration of nickel in effluent water increases from 0.32 to 0.47 mg/L. Meanwhile, the result of sludge's TCLP test increases from 3.87 to 5.23 mg/L. It is commonly known that excess OH^- could improve reducing conditions which are required for the exclusive establishment of ferrite frameworks (Wang et al. 2005). Nevertheless, in this study, the removal efficiency of nickel and the stability of sludge were restrained when the pH > 10.0. The concentration of nickel in effluent water and TCLP result of the resulting sludge present uptrend along with the increasing pH value. A possible explanation is shown in the following process:

$$Fe(OH)_2 \rightarrow Fe(OH)_3^- \rightarrow Fe(OH)_{3aq} \rightarrow FeO_m(OH)_{3-2m} \rightarrow \alpha-FeOOH$$
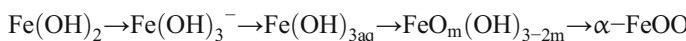
Higher pH value is not conducive to the formation of stable spinel-type structures (Wang et al. 2005). Nickel is removed in the form of hydroxide. Meanwhile, the XRD patterns in Fig. 3b exhibit that the intensity of ferrite peaks is gradually weaken when the pH value was higher than 10, confirming the inhibitory effect of pH on ferrite formation under strong alkali conditions. This result was consistent with the previous report

that ferrite formation was inhibited in the strongly alkaline solution at ambient temperature (Wang et al. 1996). With pH value from 10 to 11.2, the concentration of nickel both in effluent water and TCLP test met the Emission Standards of Pollutants for Electroplating (GB 21900 - 2008) and Identification Standards for Hazardous Wastes (GB 5085.3 - 1996), where the threshold concentration is 0.5 mg/L and 5.0 mg/L, respectively.

Ni/T-Fe ratio

The ratio of Ni/T-Fe is another important parameter affecting the removal efficiency of nickel and the stability of sludge. The concentration of divalent nickel is given by X, where X is defined in Ni/T-Fe molar ratio as $X/3-X$ based on Eq.(10). To estimate the optimal incorporation degree of nickel into the ferrite lattice at room temperature, different matching experiments were performed by RF process.

$$xNi^{2+} + (1-x)Fe^{2+} + 2Fe^{3+} + 6OH^- \rightarrow Ni_xFe_{1-x}O \cdot Fe_2O_3 + 3H_2O \tag{10}$$
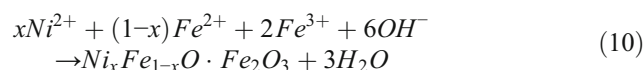
Figure 4 illustrates the downward and upward trend of the concentration of nickel both in effluent water and the sludge TCLP test. The minimum value is achieved at $X = 0.075$. It seems that this point is the threshold of concentration of nickel in RF system at ambient temperature. With the decrease of the X from 0.075 to 0.025, the concentrations of both effluent water and the sludge TCLP test increase, due to the competition between Fe(II) and Ni(II) capturing into the spinel ferrite structure (Lou et al. 2009) (see Eq. (1)). The nickel ions incorporated into the ferrite structure released into the solution again when $X = 0.025$. When X increases from 0.075 to 0.14, the concentration of nickel in effluent water and in TCLP test rise up again. Excess nickel ions, which did not incorporated into the stable and compact ferrite structure, precipitated in the
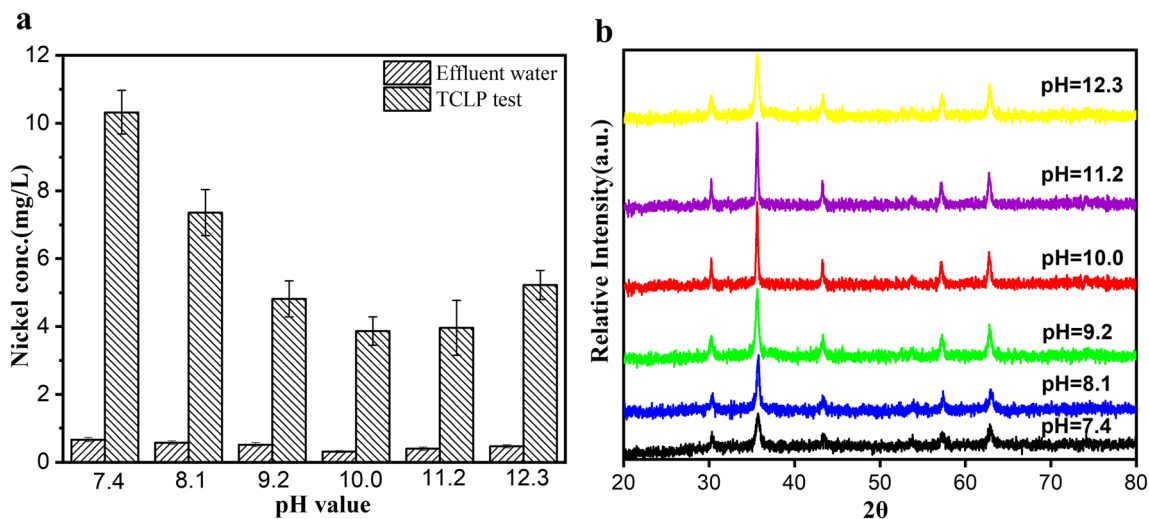

Fig. 3 **a** Effect of pH in RF reactor on the concentration of nickel in effluent water and TCLP test and **b** their XRD patterns
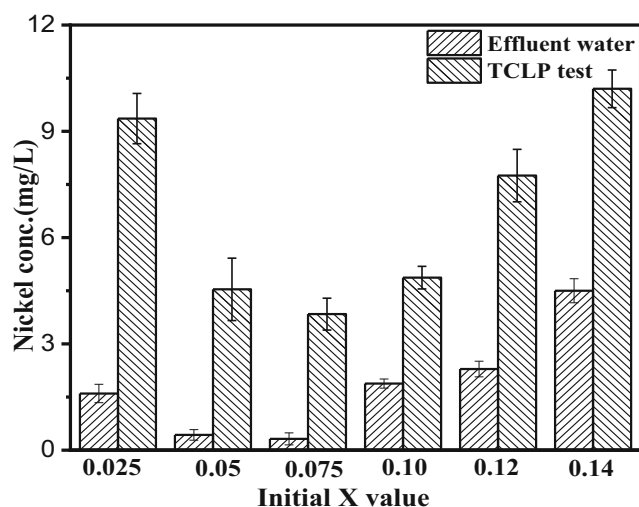
Fig. 4 Effect of initial X value on the nickel concentration of effluent water and TCLP test

form of $Ni(OH)_2$. According to the literatures, the incorporation degree of designated ratio (100% incorporation) could not be reached and the maximal degree of incorporation for nickel was $X = 0.78$ ($T > 65$ °C) (Mckinnon et al. 2000). However, Klas et al. hold the point that the maximal degree was 0.06 at ambient temperature (Klas et al. 2011). The incorporate degree at elevated temperature was higher than that at ambient temperature, because higher temperature promoted dehydration effect to form more ferrite structure.

When X was between 0.05 and 0.075, the concentrations of nickel both in effluent water and TCLP test met the Emission Standards of Pollutants for Electroplating and Identification Standards for Hazardous Wastes, respectively. However, as mentioned above, the maximal degree of nickel incorporation was 0.06 at ambient temperature. The optimal degree of nickel incorporation ($X = 0.075$) in this study was higher than 0.06 due to the wrapping and entraining by ferrite particle for residual nickel ($X = 0.075 – 0.06 = 0.015$). Therefore, $X = 0.075$, representing a lower consumption and higher removal efficiency, was chosen as the optimal value for RF process. In such condition, the amount of the Fe(II) ions which were needed in RF process were 7.43 g/L in total. Nevertheless, Fe(II) ions of 6.97 g/L were needed in RF reactor due to extra Fe(III) ions of 450 mg/L, which flowed into the RF reactor from the FO process.

Returning slurry ratio

Magnetite particles have been widely used as seeds for treating industrial wastewater (Morgan et al. 2003; Kefeni et al. 2017; Morgan et al. 2005). By integrating the seed process with the RF process, heavy metal ions existing in electroplating wastewater are likely to co-precipitate on magnetic seeds in the form of magnetic ferrite. The magnetite particles as seeds not only improve the removal efficiency of

heavy metal, but also reduce the demand of iron salts. In our research, slurry was returned to the alkaline conditioning tank for aging to form magnetic ferrites as seeds before flowing into the RF reactor. According to the literature, aging is beneficial for the crystallinity of precipitate at ambient temperature (Mckinnon et al. 2000; Oscar Perales-Perez 2002). Nevertheless, pH value has an obvious effect on aging process in alkaline conditioning tank, which will generate different products at different pH values. Oscar Perales Perez and Yoshiaki Umetsu have reported that the precipitate only showed sharp peaks of crystalline magnetite when the pH value was higher than 10. However, the main products were Green rust-II and Lepidocrocite (γ-FeOOH) when pH = 7, while products were Green rust-II, γ-FeOOH, and Amarantite ($FeSO_4(OH)\cdot 3H_2O$) when pH = 8 (Perez et al. 1998). Hence, highly purified ferrite sludge produced under higher pH value (pH > 10). In this study, as mentioned in the "pH value" section, pH value in alkaline conditioning tank was higher than 11 when RF was operated at the optimal condition. Magnetic ferrites were the main products and pH was maintained at 11.8 in alkaline conditioning tank for the following experiments.

The returning slurry ratio, which influence the residence time of slurry in alkaline conditioning tank, is one of the key factors affecting the formation of magnetic ferrite. As such, its effects on nickel concentration in effluent water and TCLP test were explored at different returning slurry ratios. Figure 5. shows that the concentrations of nickel in effluent water and TCLP test gradually decreased as the returning slurry ratio increase from 0.03 to 0.17. With the returning slurry ratio increasing from 0.03 to 0.17, the returning slurry (ferrite) as a seed material facilitated the formation of ferrite. As the returning slurry ratio increase from 0.17 to 0.25, there was almost no change of the nickel concentration which is lower than the relevant standard values both in effluent water and
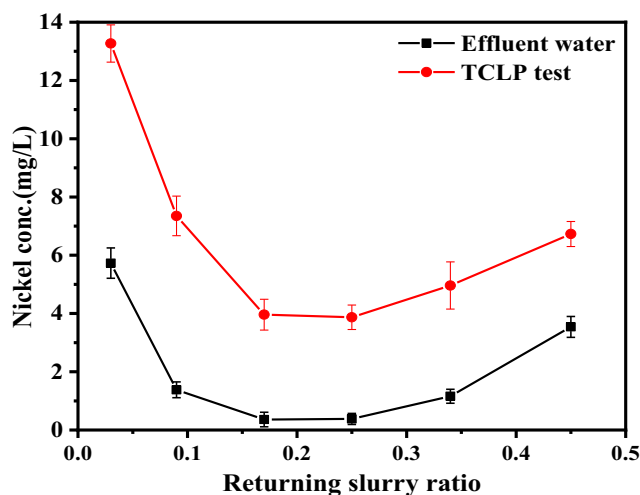

Fig. 5 Effect of returning slurry ratio on the removal efficiency of nickel and TCLP
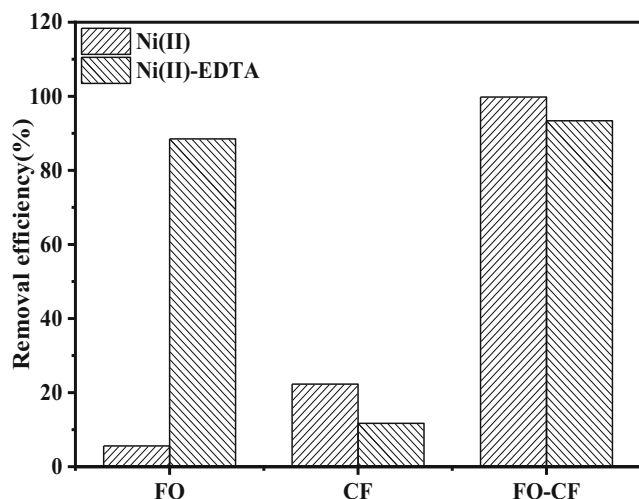
Fig. 6 Comparison of the removal efficiency in FO, RF, and FO-RF processes. (Initial pH of the FO and RF process was 2.5 and 10, respectively. $[Ni(II)]_0 = 3.40$ mM, FO process: 60 min, $Fe(II) = 450$ mg/L, $H_2O_2 = 1800$ mg/L)

TCLP test. However, with the ratio further increasing from 0.25 to 0.45, the nickel concentrations both in effluent water and TCLP test gradually rise up owing to the retention time of returning slurry, as aging is too short in alkaline conditioning tank. According to the above analysis, the optimal ratio of returning slurry can be determined between 0.17 and 0.25 for the RF system.

Comparison of FO-RF with FO and RF process

In order to evaluate the efficiency of treatment of wastewater contaning Ni(II)-EDTA in the sole FO and RF, FO-RF was compared with separate FO and RF process. Figure 6 indicates that the decomplexation of Ni(II)-EDTA is mainly completed in the FO process ($R_{Ni(II)-EDTA} = 88.5\%$) and the removal efficiency of nickel ions is 5.6% in this stage. In the RF process, $R_{Ni(II)-EDTA}$ and R_{Ni} are only 11.7% and 22.3%, respectively. It is also noted that both Ni(II) and Ni(II)-EDTA are efficiently removed in the FO-RF in contrast to the separate FO and RF process. Therefore, the decomplexation of Ni(II)-EDTA before the wastewater flow into the RF process is necessary, and it can be concluded that the FO-RF is an effective method for the treatment of wastewater containing Ni(II)-EDTA. The process involved several decomplexation in the FO process, adsorption, wrap, entrainment, and replacement in RF process

Table 2 The optimum ranges in RF process

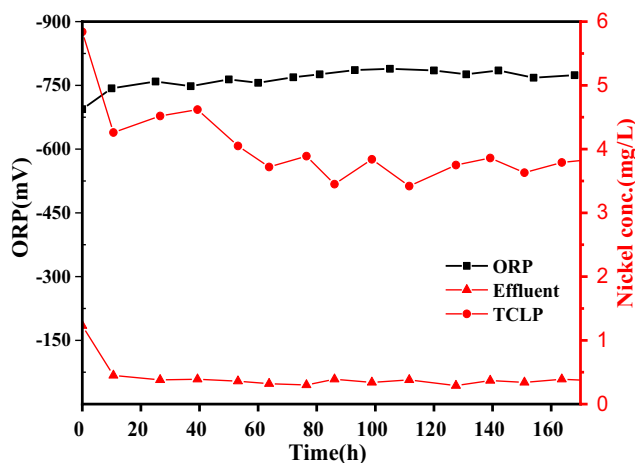| Serial number	X	pH in RF reactor	Returning slurry ratio
The optimal conditions	0.05–0.075	10.0–11.2	0.17–0.25

Fig. 7 Continuous operation under the best conditions

which was the main reason for the high removal efficiency in the FO-RF.

Optimum operating parameters

As analyzed above, as long as the main influencing factors (X, pH in RF reactor, and returning slurry ratio) maintained within a certain range, both effluent water and TCLP test satisfied Emission Standards of Pollutants for Electroplating and Identification Standards for Hazardous Wastes, respectively. The optimum ranges are shown in Table 2. In order to clearly describe the process of RF reaction, the RF reactor was monitored at set intervals under the best conditions ($X = 0.075$, pH = 10, returning slurry ratio = 0.17). The ORP in RF reactor, effluent water quality, and the stability of sludge in thickener was measured. The results indicate that the reactor is basically in a stable state after 10 h except for slight fluctuation in TCLP test (Fig. 7). Under this condition, as long as X was not excessively high, the nickel concentration in effluent water was lower than 0.4 mg/L and the ORP leveled off − 750 mV vs Ag/AgCl. The sludge was stable and TCLP satisfied relevant standards (the "The evaluation of sludge's performance" section). The resulting sludge was characterized by dark black color and exhibited a strong magnetic field.

The evaluation of sludge's performance

TCLP

Table 3 shows the leachability of nickel in TCLP test at ambient temperature by traditional alkaline precipitation and FO-

Table 3 Sludge leaching test results (mg/L)

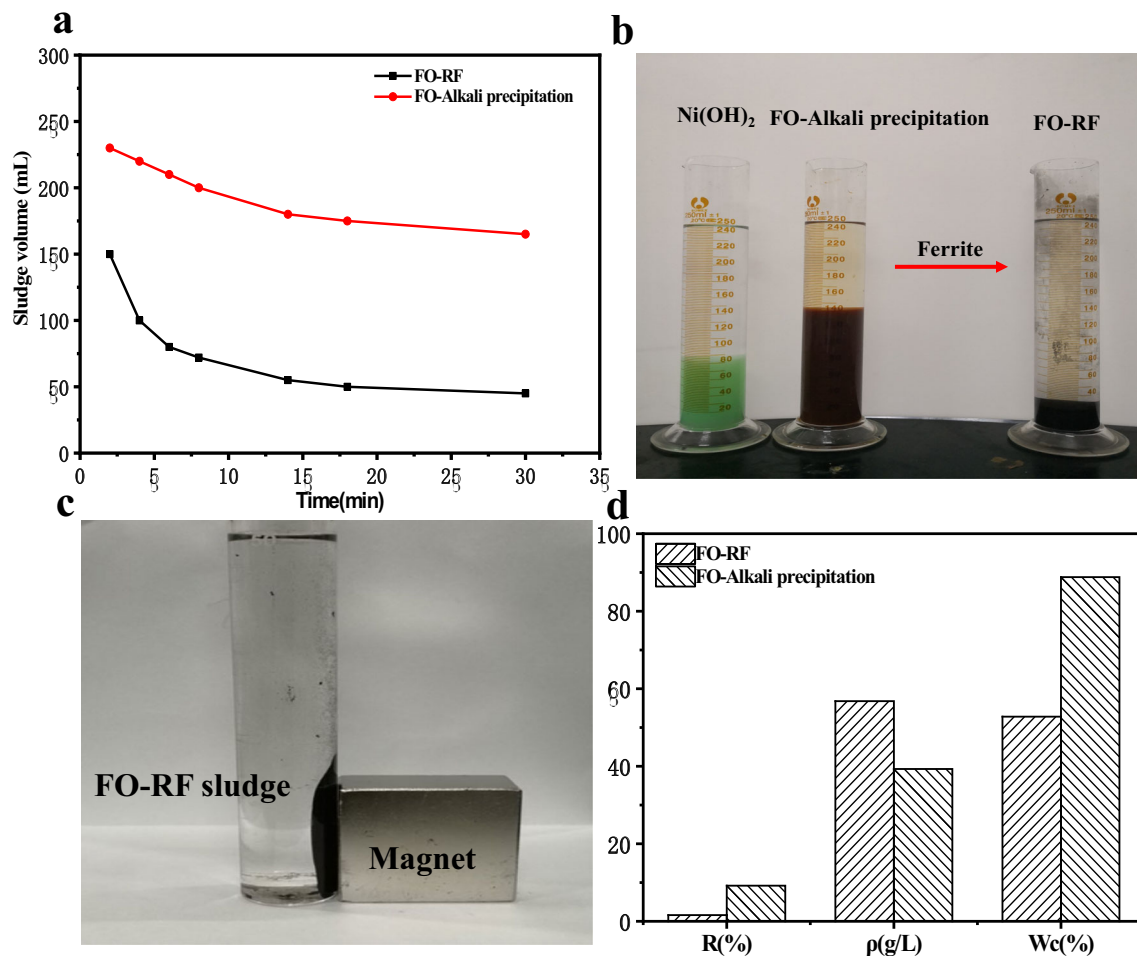|	Standard (China)	Ni(OH)$_2$	FO-RF
Nickel	5	420–516	2.81–4.08

Fig. 8 The performance of the FO-RF sludge. **a** The change of sludge volume over time by FO-RF and alkali precipitation after FO process. **b** The sludge settling situation after 60 min by Ni(OH)$_2$, FO-Alkali precipitation, and FO-RF, respectively. (Initial volume, 250 mL; [Ni(II)]$_0$ = 3.40 mM). **c** The separation for FO-RF sludge by using an external magnetic field within 10 s. **d** Sludge performance evaluation: stable sludge volume ratio (R), compressed solid concentration (ρ), and water content (Wc), respectively
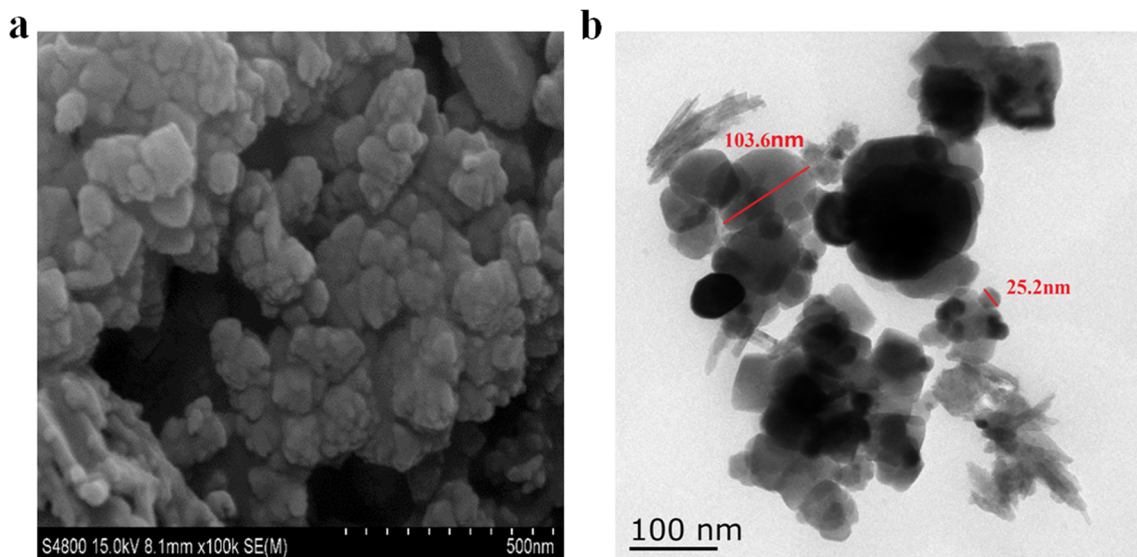

Fig. 9 **a** SEM and **b** TEM images of the resulting sludge generated by the FO-RF process

Table 4 EDS test results of the resulting sludge generated from the FO-RF

Element	O	Fe	Ni
Atomic (mol%)	56.91	42.13	0.93

RF process. The experimental data indicates that the nickel ions are less mobile in the generated ferrite-bearing sludge than in the $Ni(OH)_2$. In other words, the result of TCLP test can meet Identification Standards for Hazardous Wastes. On the contrary, $Ni(OH)_2$ was completely dissolved under weak acid conditions in the TCLP test. The concentration of nickel ions which dissolved in the TCLP test was double than initial concentration (200 mg/L).

The chemical stability of the sludge, which may have major implications on the final treatment of the product, reflects the stable degree of the heavy metals. It is generally accepted that dehydration is a crucial step in ferrite formation. In the conventional approach, in order to fulfill the TCLP demands, much longer time was required for attaining final stable precipitate (Bemorga et al. 2005). The ferrite reaction can be promoted at elevated temperature for the reason that the dehydration rate is associated with the temperature. However, elevated temperature increased treatment costs. In this research, returning slurry was returned to the alkaline conditioning tank for aging which was conducive to the formation of ferrite in the FO-RF process (in the "Returning slurry ratio" section). It showed a high efficiency of nickel removal in a short period of time. The dissolution rates of heavy metals were also lower than traditional method at ambient temperature.

Compactness and moisture content of the sludge

Figure 8a exhibits the change of sludge volume over time by FO-RF and FO-Alkali precipitation. It can be found that the settling velocity of FO-RF sludge was obviously faster than traditional alkaline precipitation sludge. After 14 min, the volume of ferrite was reduced by 80%, and those of FO-Alkali precipitation were reduced only by 34%. In order to explain the impact of the RF on FO-RF process, the volume change of $Ni(OH)_2$, FO-Alkali precipitation, and FO-RF sludge was investigated after 60 min. The results suggest that the volume of FO-Alkali precipitation is 1.75 times higher than $Ni(OH)_2$ (Fig. 8b). Nevertheless, in contrast, the volume of RF sludge after FO process is almost 7 times lower than alkali precipitation which is after FO process. Meanwhile, it is also 4 times lower than $Ni(OH)_2$. Therefore, RF facilitates the densification of the sludge after FO process. In addition, an external magnetic field can be used in quick separation for FO-RF sludge due to its soft magnetism (Fig. 8c), and the time is much less than those of sedimentation technique.

To further evaluate the performance of sludge, stable sludge volume ratio (R), compressed solid concentration (ρ), and water content (W_c) were discussed. The result from Fig. 8d displays that volume ratio (R), compressed solid concentration (ρ), and water content (W_c) of the FO-RF resulting sludge are 1.6%, 56.8 mg/L, and 52.8%, respectively. Meanwhile, the sedimentation velocity of FO-RF is 2.16 times faster than the conventional alkaline precipitation, demonstrating the excellent sludge performance of FO-RF.

SEM, EDS, and TEM measurement

The images of scanning electron micrograph (SEM) and transmission electron micrograph (TEM) are shown in Fig. 9. Through the SEM test, it could be clearly observed that the resulting sludge is composed of granular particle. In order to gauge the particle size of the resulting sludge, TEM was also used. The particle size was calculated using a line sectioning method. Figure 9 b presents the TEM image of the sludge. The particle size is approximately at 25.2–103.6 nm. Table 4 shows the EDS test results, it is revealed that the major elements of the resulting sludge are Ni, Fe, and O, and the structural formula of the resulting sludge can be expressed using $Ni_{0.064}Fe_{2.936}O_4$ ($X = 0.064$).

Conclusions

In this study, the FO-RF procedure was proposed as a promising method for treating electroplating wastewater containing Ni(II)-EDTA complexes under ambient temperature. The conclusions of this research are shown as follows:

1. The optimum reaction conditions for the FO process were as follows: Fe(II) dosage of 450 mg/L and H_2O_2 dosage of 1800 mg/L at pH of 2.5. In this conditions, the efficiency of decomplexation for Ni(II)-EDTA was nearly 88.5%.
2. The best conditions for nickel removal by RF system included a pH of 10, $X = 0.075$, and returning slurry ratio was 0.17. Following above optimal operating parameters, 99.8% Ni(II) and 93.4% Ni(II)-EDTA were removed by the FO-RF process.
3. The sludge performance results indicated that the FO-RF resulting sludge is superior to the conventional alkaline precipitation in terms of settleability and stability.
4. The combined process of FO and RF has great potential for the degradation of non-biodegradable wastewater containing Ni(II)-EDTA due to its low-cost, high efficiency, and easy operation.

References

Morgan BE, Lahav O, Loewenthal, RE (2005) Advances in seeded ambient temperature ferrite formation for treatment of acid mine drainage. Environ Sci Technol 7678–7683

Chandra S, Patel MD, Lang H, Bahadur D (2015) Dendrimer-functionalized magnetic nanoparticles: a new electrode material for electrochemical energy storage devices. J Power Source 280:217–226

Chen M, Zhou J, Zhang J, Zhang J, Chen Z, Ding J, Kong F, Qian G, Chen J (2017a) Ferrite catalysts derived from electroplating sludge for high-calorie synthetic natural gas production. Appl Catal A-Gen 534:94–100

Chen Y, Zhao X, Guan W, Cao D, Guo T, Zhang X, Wang Y (2017b) Photoelectrocatalytic oxidation of metal-EDTA and recovery of metals by electrodeposition with a rotating cathode. Chem Eng J 324:74–82

Cunha Gda C, Goveia D, Romao LP, de Oliveira LC (2015) Effect of the competition of Cu(II) and Ni(II) on the kinetic and thermodynamic stabilities of Cr(III)-organic ligand complexes using competitive ligand exchange (EDTA). J Environ Manag 154:259–265

Dar MA, Majid K, Najar MH, Kotnala RK, Shah J (2016) Synthesis and characterization of $Li_{0.5}Fe_{2.5-x}Gd_xO_4$ ferrite nano-particles as a potential candidate for microwave device applications. Mater Des 90:443–452

Erdem M, Tumen F (2004) Chromium removal from aqueous solution by the ferrite process. J Hazard Mater 109:71–77

Fu F, Wang Q, Tang B (2009) Fenton and Fenton-like reaction followed by hydroxide precipitation in the removal of Ni(II) from NiEDTA wastewater: a comparative study. Chem Eng J 155:769–774

Fu F, Xie L, Tang B, Wang Q, Jiang S (2012) Application of a novel strategy—advanced Fenton-chemical precipitation to the treatment of strong stability chelated heavy metal containing wastewater. Chem Eng J 189-190:283–287

Guivar JA, Fernandes EG, Zucolotto V (2015) A peroxidase biomimetic system based on Fe_3O_4 nanoparticles in non-enzymatic sensors. Talanta 141:307–314

Han Y, Li H, Liu M, Sang Y, Liang C, Chen J (2016) Purification treatment of dyes wastewater with a novel micro-electrolysis reactor. Sep Purif Technol 170:241–247

Hasanzadeh M, Shadjou N, de la Guardia M (2015) Iron and iron-oxide magnetic nanoparticles as signal-amplification elements in electrochemical biosensing. Trac Trend Anal Chem 72:1–9

Huang Y-H, Wang S-F, Tsai A-P, Kameoka S (2015) Catalysts prepared from copper–nickel ferrites for the steam reforming of methanol. J Power Sources 281:138–145

Jiang T, Liang Y-d, He Y-j, Wang Q (2015) Activated carbon/$NiFe_2O_4$ magnetic composite: a magnetic adsorbent for the adsorption of methyl orange. J Environ Chem Eng 3:1740–1751

Ju F, Hu Y (2011) Removal of EDTA-chelated copper from aqueous solution by interior microelectrolysis. Sep Purif Technol 78:33–41

Kefeni KK, Mamba BB, Msagati TAM (2017) Magnetite and cobalt ferrite nanoparticles used as seeds for acid mine drainage treatment. J Hazard Mater 333:308–318

Kim HT, Lee TG (2017) A simultaneous stabilization and solidification of the top five most toxic heavy metals (Hg, Pb, As, Cr, and Cd). Chemosphere 178:479–485

Kim SJ, Lim KH, Joo KH, Lee MJ, Kil SG, Cho SY (2002) Removal of heavy metal-cyanide complexes by ion exchange. Korean J Chem Eng 19:1078–1084

Klas S, Dubowski Y, Lahav O (2011) Chemical stability and extent of isomorphous substitution in ferrites precipitated under ambient temperatures. J Hazard Mater 193:59–64

Koo D-S, Sung H-H, Kim S-S, Kim G-N, Choi J-W (2017) Characteristics of cement solidification of metal hydroxide waste. Nucl Eng Technol 49:165–171

Lan S, Ju F, Wu X (2012) Treatment of wastewater containing EDTA-Cu(II) using the combined process of interior microelectrolysis and Fenton oxidation–coagulation. Sep Purif Technol 89:117–124

Li L, Huang Z, Fan X, Zhang Z, Dou R, Wen S, Chen Y, Chen Y, Hu Y (2017) Preparation and characterization of a Pd modified Ti/SnO_2-Sb anode and its electrochemical degradation of Ni-EDTA. Electrochim Acta 231:354–362

Liu F, Shan C, Zhang X, Zhang Y, Zhang W, Pan B (2017) Enhanced removal of EDTA-chelated cu(II) by polymeric anion-exchanger supported nanoscale zero-valent iron. J Hazard Mater 321:290–298

Lou JC, Huang YJ (2009) Assessing the performance of wastewater treatment with the combination of Fenton and ferrite process. Environ Monit Assess 151:251–258

Lou JC, Huang YJ, Han JY (2009) Treatment of printed circuit board industrial wastewater by ferrite process combined with Fenton method. J Hazard Mater 170:620–626

Mckinnon W, Choung JW, Xu Z, Finch JA (2000) Magnetic seed in ambient temperature ferrite process applied to acid mine drainage treatment. Environ Sci Technol 2576–2581

Morgan BE, Lahav O, Hearne GR, Loewenthal RE (2003) A seeded ambient temperature ferrite process for treatment of AMD waters magnetite formation in the presence and absence of calcium ions under steady state operation. Water SA 29:117–124

Morgan BE, Loewenthal RE, Lahav O (2004) Fundamental study of a one-step ambient temperature ferrite process for treatment of acid mine drainage waters: rapid communication. Water SA 27:277–282

Oscar Perales-Perez YU (2002) Ambient-temperature precipitation of Zn ions from aqueous solutions as ferrite-type compounds. Hydrometallurgy 63:235–248

Perez OP, Umetsu Y, Sasaki H (1998) Precipitation and densification of magnetic iron compounds from aqueous solutions at room temperature. Hydrometallurgy 50:223–242

Qiu B, Li Q, Shen B, Xing M, Zhang J (2016) Stöber-like method to synthesize ultradispersed Fe_3O_4 nanoparticles on graphene with excellent photo-Fenton reaction and high-performance lithium storage. Appl Catal B Environ 183:216–223

Qu J, Che T, Shi L, Lu Q, Qi S (2019) A novel magnetic silica supported spinel ferrites $NiFe_2O_4$ catalyst for heterogeneous Fenton-like oxidation of rhodamine B. Chin Chem Lett

Rincon GJ, La Motta EJ (2014) Simultaneous removal of oil and grease, and heavy metals from artificial bilge water using electro-coagulation/flotation. J Environ Manag 144:42–50

ShinJuang R, ChunLin L (2001) Electrochemical treatment of copper from aqueous citrate solutions using a cation-selective membrane. Sep Purif Technol 22-2:627–635

ShinJuang R, WenWang S, ChunLin L (1999) Simultaneous recovery of EDTA and lead(II) from their chelated solutions using a cation exchange membrane. J Membrane Sci 160:225–233

Wang J, Deng T, Dai Y (2005) Study on the processes and mechanism of the formation of Fe_3O_4 at low temperature. J Alloy Compd 390:127–132

Wang W, Xu Z, Finch, J (1996) Fundamental study of an ambient temperature ferrite process in the treatment of acid mine drainage. Environ Sci Technol 30:2604–2608

Wu L, Wang H, Lan H, Liu H, Qu J (2013) Adsorption of Cu(II)–EDTA chelates on tri-ammonium-functionalized mesoporous silica from aqueous solution. Sep Purif Technol 117:118–123

Xu Z, Gao G, Pan B, Zhang W, Lv L (2015) A new combined process for efficient removal of Cu(II) organic complexes from wastewater:

Fe(III) displacement/UV degradation/alkaline precipitation. Water Res 87:378–384

Xu Z, Shan C, Xie B, Liu Y, Pan B (2017) Decomplexation of Cu(II)-EDTA by UV/persulfate and UV/H$_2$O$_2$: efficiency and mechanism. Appl Catal B Environ 200:439–447

Yi J, She X, Song Y, Mao M, Xia K, Xu Y, Mo Z, Wu J, Xu H, Li H (2018) Solvothermal synthesis of metallic 1T-WS$_2$: a supporting co-catalyst on carbon nitride nanosheets toward photocatalytic hydrogen evolution. Chem Eng J 335:282–289

Yi J, Li H, Gong Y, She X, Song Y, Xu Y, Deng J, Yuan S, Xu H, Li H (2019a) Phase and interlayer effect of transition metal dichalcogenide cocatalyst toward photocatalytic hydrogen evolution: the case of MoSe$_2$. Appl Catal B-Environ 243:330–336

Yi J, Liao J, Xia K, Song Y, Lian J, She X, Liu Y, Yuan S, Dong F, Xu H, Li H (2019b) Integrating the merits of two-dimensional structure and heteroatom modification into semiconductor photocatalyst to boost NO removal. Chem Eng J 370:944–951

Zhou D, Hu Y, Guo Q, Yuan W, Deng J, Dang Y (2016) Decomplexation efficiency and mechanism of Cu(II)-EDTA by H$_2$O$_2$ coupled internal micro-electrolysis process. Environ Sci Pollut Res 26:1015–1025